J. Membrane Biol. 149, 89–101 (1996)

The Journal of
Membrane
Biology

Modeling the Current-Voltage Characteristics of *Chara* Membranes: I. The Effect of ATP Removal and Zero Turgor

M.J. Beilby, N.A. Walker
School of Physics, Biophysics, University of NSW, Kensington 2052, NSW, Australia

Received: 23 January/Revised: 10 October 1995

Abstract: We have obtained and modeled the electrical characteristics of the plasma membrane of *Chara* internodal cells: intact, without turgor and perfused with and without ATP. The cells were voltage and space-clamped to obtain the *I/V* (current-voltage) and *G/V* (conductance-voltage) profiles of the cell membrane.

The intact cells yielded similar *I/V* characteristics with resting p.d.s of −221 ± 12 mV (cytoplasmic clamp, 5 cells) and −217 ± 12 mV (vacuolar clamp, 5 cells). The cut unperfused cells were depolarized at −169 ± 12 mV (7 cells) compared to the vacuole-clamped intact cells. The cells perfused with ATP fell into three groups: hyperpolarized group with resting p.d. −175 ± 12 mV (4 cells) and *I/V* profile similar to the intact and cut unperfused cells; depolarized group with resting p.d. of −107 ± 12 mV (6 cells) and *I/V* profiles close to linear; and excited cells with profiles showing a negative conductance region and resting p.d. at −59 ± 12 mV (5 cells). The cells perfused with medium containing no ATP showed upwardly concave *I/V* characteristics and resting p.d. at −81 ± 12 mV (6 cells).

The *I/V* curves were modeled employing the ''Two-state'' model for the H^+ pump (Hansen et al., 1981). The inward and outward rectifiers were fitted to exponential functions and combined with a linear background current. The excitation state in perfused cells was modeled by including an inward current, i_{excit}, with p.d.-dependence described by a combination of hyperbolic tangent functions. An inward current, $i_{no\text{-}ATP}$, with a smaller amplitude, but very similar p.d.-dependence was also included in the simulation of the *I/V* curves from cells without ATP. This approach avoided *I/V* curve subtraction.

The modeling of the total *I/V* and *G/V* characteristics provided more information about the parameters of the ''Two-state'' pump model, as well as more quantitative understanding of the interaction of the major transport systems in the plasmalemma in generation of the resting potential under a range of circumstances. ATP had little effect on nonpump currents except the excitation current; depolarization profoundly affected the pump characteristics.

Key words: Pump modeling — Effect of ATP — *Chara* — Current-voltage profiles — Excitation — Perfusion

Introduction

Since it has been realized that the resting p.d. in plant cells consists of an active, ATP-driven potential and a diffusive passive potential due to asymmetrical distribution of ions in the various compartments, many experiments have been designed to quantify the contributions of the various transport systems (*see* Hope & Walker, 1975, for historical account). The task is made more difficult by the complex voltage dependencies of some of the transporters. More than ten years ago Beilby and Beilby (1983) showed that under a range of conditions the *I/V* characteristics of the *Chara* plasmalemma are sigmoid with a conductance maximum near the resting potential. In the following years there have been several attempts (Kishimoto et al., 1984; Beilby, 1984; Takeuchi et al., 1985) to fit such *I/V* profiles to HGSS[1] model describing the kinetics of the H^+-extruding ATPase (Hansen et al., 1981). The different values of reaction constants and H^+/ATP stoichiometry obtained by differ-

Correspondence to: M.J. Beilby

[1] The acronym is derived from the first letters of the surnames of the authors: Hansen, Gradmann, Sanders and Slayman

ent workers foreshadowed how fraught with difficulty the isolation of the pump electrical characteristics will be. Blatt (1986) elegantly summarized the range of pitfalls from the more obvious nonspecificity of various metabolic inhibitors to the more obscure effects of asymmetry of the pump inhibition. Blatt, Beilby and Tester (1990) attempted yet another fitting of the HGSS model with these pitfalls in mind. As did Beilby (1984), they concluded that the pump stoichiometry was $1H^+/1ATP$, but they placed the pump equilibrium at more negative p.d. near −420 mV (compared to Beilby's values ranging from −110 mV at pH_o 4.5 to −330 mV at pH_o 8.5). Further, rather than assigning the pump *I/V* the simple hyperbolic tangent shape with conductance maximum near the reversal p.d., they postulated that the voltage-dependent transition does not dominate the reaction and the *I/V* curve exhibits a conductance maximum on the depolarized side of the reversal p.d. and a very broad voltage range (*see* Hansen et al., 1981, for mathematical analysis). Interestingly, a similar fit of the model could be made to the H^+ pump in *Vicia* guard cells (Blatt, 1987). A negative reversal p.d. of −450 mV for the proton pump was also obtained in *Chara* acid bands using voltage clamp to control membrane p.d. and the vibrating probe to measure external current (Fisahn & Lucas, 1992). The shape of the *I/V* curve, however, was somewhat different from that recorded by Blatt, Beilby and Tester (1990). It is not clear why the current through the hyperpolarized Cl^- channels (Tyerman, Findlay & Paterson, 1986*a*) did not swamp the pump current at such negative p.d.s. This current should be detectable by the vibrating probe as it rises exponentially near −200 mV at pH_o similar to that found in the acid zones (Tyerman, Findlay & Paterson, 1986*b*). Fisahn, Hansen and Lucas (1992) proposed a two-loop slip model which accommodates both the acid and the alkaline band *I/V* profile. While it is possible that the proton pump turns into a H^+/OH^- channel at high pH, the model is not convincing, as more parameters than experimental points seem to be needed to fit both sets of data.

In this investigation, we have approached the problem from another direction. It was hoped that the direct control of concentrations of ATP (pump energy source), ADP and P_i in the cytoplasmic compartment would avoid modification of other transporters and prevent the pump contributions from ''running in reverse'' (Chapman, Johnson & Kootsey, 1983), thus making the ''true'' difference *I/V* curve attainable. Smith and Walker (1981) made the first attempt to investigate the *I/V* characteristics of the proton pump while controlling the composition of the cytoplasm using the perfusion technique, but their *I/V* curve segments were too short to attempt fitting of the HGSS model. Thus the original aim of our investigation was to revisit some of the Smith and Walker (1981) experiments and measure detailed difference profiles (*I/V* with ATP — *I/V* without ATP) over a wide p.d. window. However, upon obtaining the no-ATP *I/V* characteristics we realized that, like metabolic inhibitors, ATP affects several transporters at the plasmalemma. To utilize the enormous amount of data available to us, most of the *I/V* characteristics have been modeled by a combination of the ''Two-state'' HGSS model for the H^+ pump, linear background current, and inward and outward rectifiers with exponential p.d.-dependence. The excitation inward current present in the depolarized cells perfused with ATP and in cells perfused without ATP was quantified by a combination of hyperbolic tangent functions. This approach enabled us to reevaluate many of the past experimental studies and gave us a more quantitative insight into the complex interaction of various transporters in producing the resting potential. We also obtained information on the effect of ATP on the components of the inward excitation current.

Table 1. Experimental media

Perfusion medium	
Component	Concentration/mM
KOH	60
NaCl	3
Sorbitol	100
$MgSO_4$	2
TES	110
EGTA	10
Corresponding outside medium	
NaCl	3
MES	4
Sorbitol	210
$Ca(OH)_2$	0.5
KCl	0.1

The perfusion medium was made in two lots: as above and with the double concentration of sorbitol. The concentration of sorbitol was then increased (by blending the two solutions) until the cells just plasmolyzed upon exposure to it. ATP was added as 22 mg/ml of the perfusion medium (This works out approximately as 40 mM, depending on the type of the ATP salt used. However, the effective concentration was determined by the concentration of $MgSO_4$). The pH of the media was adjusted to 7.0 with NaOH and MES.

Materials and Methods

The results were obtained in 1990-92 in the NA Walker laboratory, (Sydney University). *Chara corallina* (Klein ex Wild em. R.D.W.) was used for the experiments. The perfusion method is described in detail elsewhere (Beilby, Mimura & Shimmen, 1996). Briefly, the cell holder was designed to combine open-end perfusion and space clamp. It consisted of three chambers connected by a groove. A cell was laid along the groove and the chambers insulated by grease barriers. Perfusion medium (*see* Table 1) was introduced into the outer chambers and the outside medium (*see* Table 1) into the middle chamber. The high p.d.-measuring electrode was dipped into one of the outside chambers, the reference electrode into the middle chamber. The ends of the cell were cut and the wire was introduced through the cut end of the cell to extend throughout the middle compartment. To perfuse the cell, the

perfusing medium was added to one of the outer chambers with a pipette, while the level of perfusion medium in the other outer chamber was kept constant by aspiration. The effective ATP concentration was determined by the concentration of Mg^{2+} (*see* Table 1). In our experiments, we aimed to contrast the pump in fully operative and totally inactivated states. We therefore set the Mg.ATP concentration well into the saturation region of the ATP-dependent p.d. (Mimura, Shimmen & Tazawa, 1983).

The intact cells were voltage and space-clamped by inserting a wire along the cell axis, as described before (Beilby, 1990). The membrane p.d. was measured by insertion of microelectrodes into the cytoplasmic or vacuolar compartment.

Electrical Apparatus

The electrical apparatus has been described in detail previously (Beilby, 1990). The cells were clamped to a bipolar staircase protocol generated by LSI 11/73 with pulses of 70 msec separated by 200 msec at the resting p.d. level. The data-logging of each *I/V* scan took 8 sec. Polynomials were fitted to the *I/V* curves (three points at a time) and the *G/V* profiles were calculated by differentiation.

The Model

The whole currents flowing across plasmalemma or plasmalemma and tonoplast in series were modeled to avoid artefacts stemming from the current subtractions. To interpret our results we consider a range of *Chara* transport systems which are most likely to dominate the *I/V* and *G/V* characteristics. We used the ''Two-state'' HGSS proton pump model:

$$i_p = zFN\frac{k_{io}\kappa_{oi} - k_{oi}\kappa_{io}}{k_{io}+k_{oi}+\kappa_{io}+\kappa_{oi}} \quad (1)$$

where

$$k_{io} = k^o_{io}\, e^{zFV/2RT} \;\; (1a) \;\; \text{and} \;\; k_{oi} = k^o_{oi}\, e^{-zFV2RT} \quad (1b)$$

F,*R*,*T* have their usual meaning, *z* is the pump stoichiometry, which has been set to 1. *N* is a scaling factor ($=2\times10^{-8}$) and *V* is the p.d. across the plasmalemma or, in some cases, across both plasmalemma and tonoplast. While the number of carrier states is likely to be greater, the model for the *I/V* analysis can be reduced to a pair of p.d.-dependent rate constants, k_{io}, k_{oi} (which employ symmetric Eyring barrier) and p.d.-independent constants, κ_{io}, κ_{oi} (Hansen et al., 1981). As we are fitting the total membrane *I/V* relationship, there is insufficient information to describe higher state models. Using the parameter values from Blatt, Beilby, and Tester (1990), the response of the Two-state pump model to change in each parameter is shown in Figs. 1 to 4. It is apparent from Figs. 1 and 2 that with the pump parameters near the Blatt, Beilby and Tester (1990) values, the decrease in k^0_{io} and the increase in k^0_{oi} both move the conductance maximum in the depolarizing direction. However, in the case of k^0_{io} the conductance maximum becomes wider, whereas in the case of k^0_{oi} it becomes sharper. Consequently, it is possible to distinguish which of the parameters is changing. Figure 4 shows that the effect of change in κ_{oi} is also unambiguous. From Fig. 3 it is obvious that κ_{io} is small compared to κ_{oi} (*see also* Blatt, Beilby and Tester, 1990). The sphere of influence for this parameter lies at p.d. values too negative to be accessible.

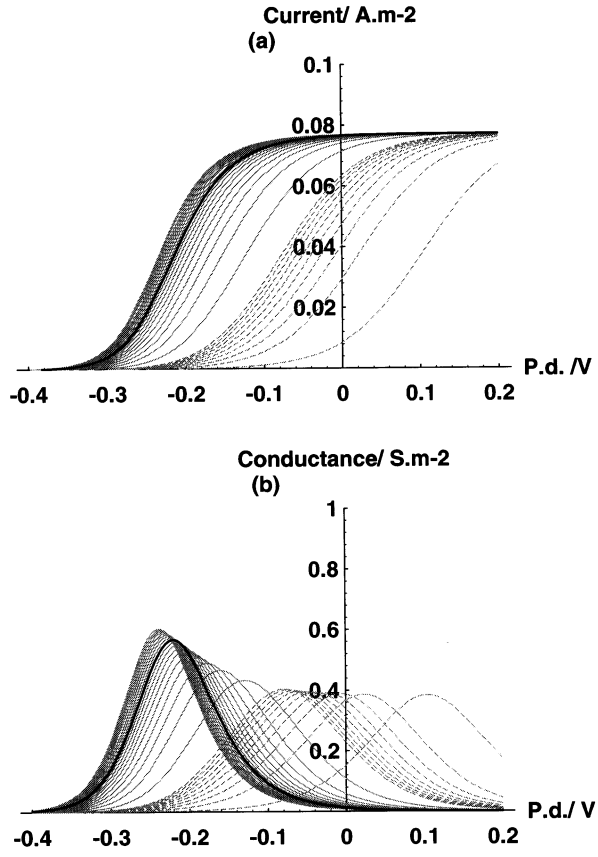

Fig. 1. The HGSS ''Two-state'' model (*see* Materials and Methods, Eqs. 1, 1*a* and *b*): the response of the *I/V* profile (*a*) and the *G/V* profile (*b*) to variation of the parameter k^0_{io} from 9000 to 5 sec^{-1}. (9000 to 500 with stepsize 500, continuous lines; 200 to 5, stepsize 20, broken lines). The other parameter values: $k^0_{oi} = 0.5$ sec^{-1}, $\kappa_{io} = 0.1$ sec^{-1}, $\kappa_{oi} = 40$ sec^{-1}. The heavy line is drawn at $k^0_{io} = 5000$ sec^{-1}. The reversal potential at the extreme values of k^0_{io}: E_p (9000) = −397 mV and E_p (5) = −209 mV. Note the evolution of the shape of the conductance maximum as k^0_{io} value decreases.

The background[2] current was approximated by a linear profile with zero current at −100 mV:

$$i_{background} = g_{background}(V + 100) \quad (2)$$

The experimental evidence for such a background current comes from several varied sources. The *I/V* profiles under metabolic blockade tend to be linear (e.g., Beilby, 1984; Blatt, Beilby & Tester, 1990). Tsutsui and Ohkawa (1993) obtained a near linear *I/V* characteristic using sulfhydryl modifying reagent NEM. Beilby and MacRobbie (1984) found a linear background current upon exposure to a calmodulin antagonist TFP. When the cells are in the K^+ state, a decrease of $[K^+]_o$ or block with TEA (Beilby, 1985, 1986) also yields linear *I/V* characteristics with similar conductance and reversal p.d. The slow-growing

[2] This current is often referred to as ''leakage'' or ''leak'' current. However, such a term implies nonspecificity and consequently reversal p.d. at 0. The reversal p.d. of −100 mV suggests some selectivity, hence the term ''background.''

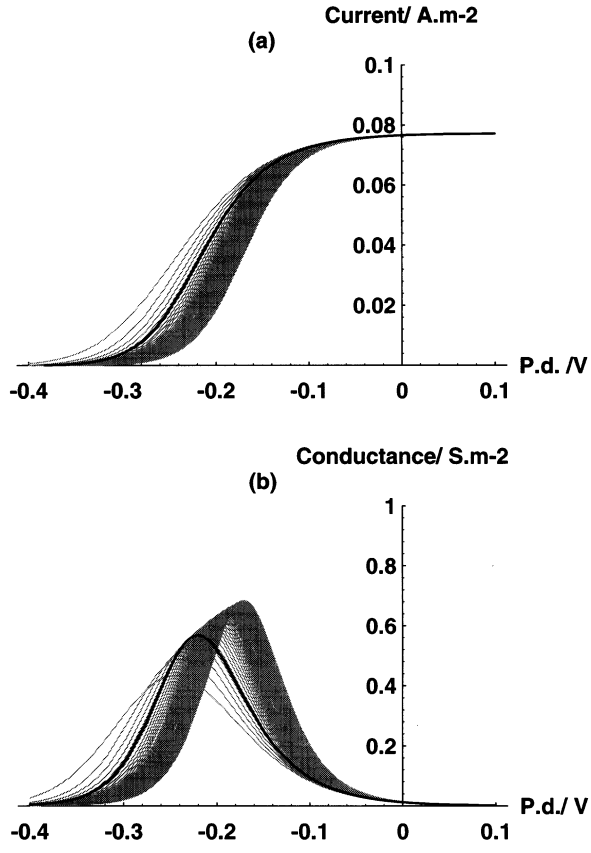

Fig. 2. The HGSS ''Two-state'' model (*see* Materials and Methods, Eqs. 1, 1*a* and *b*): the response of the *I/V* profile (*a*) and the *G/V* profile (*b*) to variation of the parameter k^0_{oi} from .05 to 5 sec^{-1} (stepsize 0.1). The other parameter values: $k^0_{io} = 5000\ sec^{-1}$, $\kappa_{io} = 0.1\ sec^{-1}$, $\kappa_{oi} = 40\ sec^{-1}$. The heavy line is drawn at $k^0_{oi} = 0.5\ sec^{-1}$. The reversal potential at the extreme values of k^0_{oi}: E_p (5.0) = −325 mV and E_p (0.05) = −441 mV. Note the evolution of the shape of the conductance maximum as k^0_{oi} value decreases.

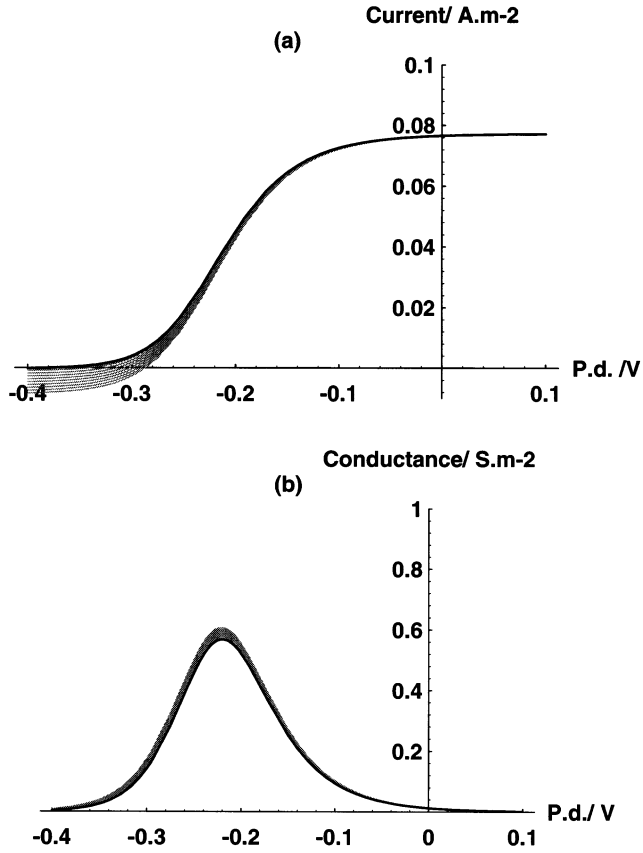

Fig. 3. The HGSS ''Two-state'' model (*see* Materials and Methods, Eqs. 1, 1*a* and *b*): the response of the *I/V* profile (*a*) and the *G/V* profile (*b*) to variation of the parameter κ_{io} from .01 to 5 sec^{-1} (stepsize 0.5). The other parameter values: $k^0_{io} = 5000\ sec^{-1}$, $k^0_{oi} = 0.5\ sec^{-1}$, $k_{oi} = 40 sec^{-1}$. The heavy line is drawn at $\kappa_{io} = 0.1\ sec^{-1}$. The reversal potential at the extreme values of κ_{io}: E_p (0.01) = −440 mV and E_p (5) = −284 mV.

Chara cells often exhibit low plasmalemma p.d.s (Shepherd & Goodwin, 1992) and linear *I/V* profiles (M.J. Beilby, *unpublished results*). The ions constituting the background current are thought to be K^+ (uninhibitable K^+ transport as described by Smith, Walker & Smith, 1987), H^+ (or OH^-) contributed by the high pH channels active in alkaline bands of the cell and possibly some Na^+. K^+ alone would have a more negative reversal p.d. Blatt, Beilby and Tester (1990) lumped the background current and the outward rectifier into a single equation. We treat the outward rectifier and the linear background current as separate transport systems. This approach is indicated by the patch clamp data from higher plants, where the outward rectifier channels have been identified (e.g., Schroeder, 1989; Terry, Tyerman & Findlay, 1991).

The p.d. window of −450 to +50 mV is delimited by inward and outward rectifier currents, which have been modeled as exponential functions of the membrane p.d.:

$$i_{inrec} = -0.005e^{-(c_1V+c_2)} \quad (3)$$

$$i_{outrec} = 0.01e^{k_1V+k_2} \quad (4)$$

where c_1, c_2 and k_1, k_2, are constants to be fitted to the data (the aim here is to quantify the currents, rather than to fit to a specific model).

The inward rectifier current is carried by Cl^- and has been described previously by an expression very similar to Eq. (3) (Tyerman, Findlay & Paterson, 1986*a*,*b*). The outward rectifier is less well characterized, but it is thought to be carried mainly by K^+. The p.d.-dependence is clearly exponential (e.g., Beilby, 1989; Terry, Tyerman and Findlay, 1991) and consequently similar expression to Eq. (3) has been adopted.

The excitation inward current in the perfused cells has been modeled by a combination of hyperbolic tangent functions:

$$i_{excit} = a[-1 + \tanh(t_1V + t_2)]\,[-1 - \tanh(u_1V + u_2)] \quad (5)$$

where a, t_1, t_2 and u_1, u_2 are constants to be fitted. The expression is similar to Hodgkin-Huxley (HH) model for the Na^+ current, as it describes a function rising exponentially, coming to a maximum and falling exponentially. However, we felt that using HH model would be misleading here, as the inward current in perfused cells is not activated and inactivated with time.

For the inward current in the profile for cells perfused with no ATP, same expression was used

$$i_{no\text{-}ATP} = a[-1 + \tanh(t_1V + t_2)]\,[-1 - \tanh(u_1V + u_2)] \quad (6)$$

As in case of the rectifiers, Eqs. (5) and (6) aim to mathematically describe the currents, rather than to fit them to a specific model.

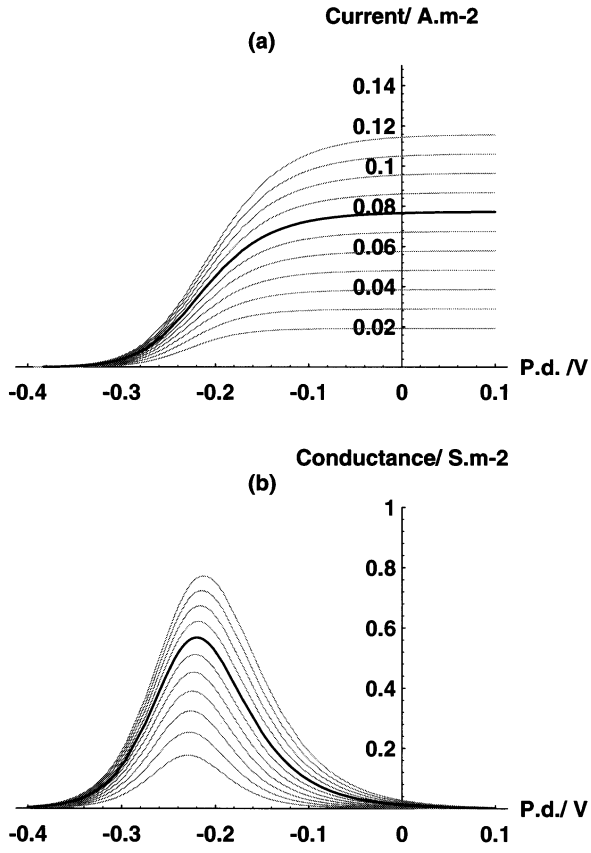

Fig. 4. The HGSS ''Two-state'' model (*see* Materials and Methods, Eqs. 1, 1*a* and *b*): the response of the *I/V* profile (*a*) and the *G/V* profile (*b*) to variation of the parameter κ_{oi} from 10 to 60 sec^{-1} (stepsize 5). The other parameter values: $k^0_{io} = 5000\ sec^{-1}$, $k^0_{oi} = 0.5\ sec^{-1}$, $\kappa_{io} = 0.1\ sec^{-1}$. The heavy line is drawn at $\kappa_{oi} = 40\ sec^{-1}$. The reversal potential at the extreme values of κ_{oi}: E_p (10.0) = −348 mV and E_p (60.0) = −446 mV.

The modeling of the data has been performed on a 486 DX2 50 PC, using Mathematica 2.2.3. A comparison with the conductances obtained from polynomial fits to the data provided additional constraints on the model. For instance, the *I/V* profile could be satisfactorily fitted with either large background current and small κ_{oi} pump model parameter or *vice versa.* However, when the model was compared to the *G/V* profile obtained by the polynomial fitting, only one of these combinations was satisfactory. The goodness of fit has been judged by eye, as in this work we aim to establish the main trends. More accurate fitting procedures will be employed as the details of the model will be worked out.

Results

To establish a ''normal'' range for the model parameters, the model was fitted to 5 intact cells with plasmalemma voltage clamped and to 5 intact cells with plasmalemma and tonoplast voltage clamped. The data and the fitted model can be seen in Figs. 5 and 6, the parameter values in Table 2. The *I/V* profiles are similar and the resting p.d.s are −221 ± 12 mV and −217 ± 12 mV, respectively.

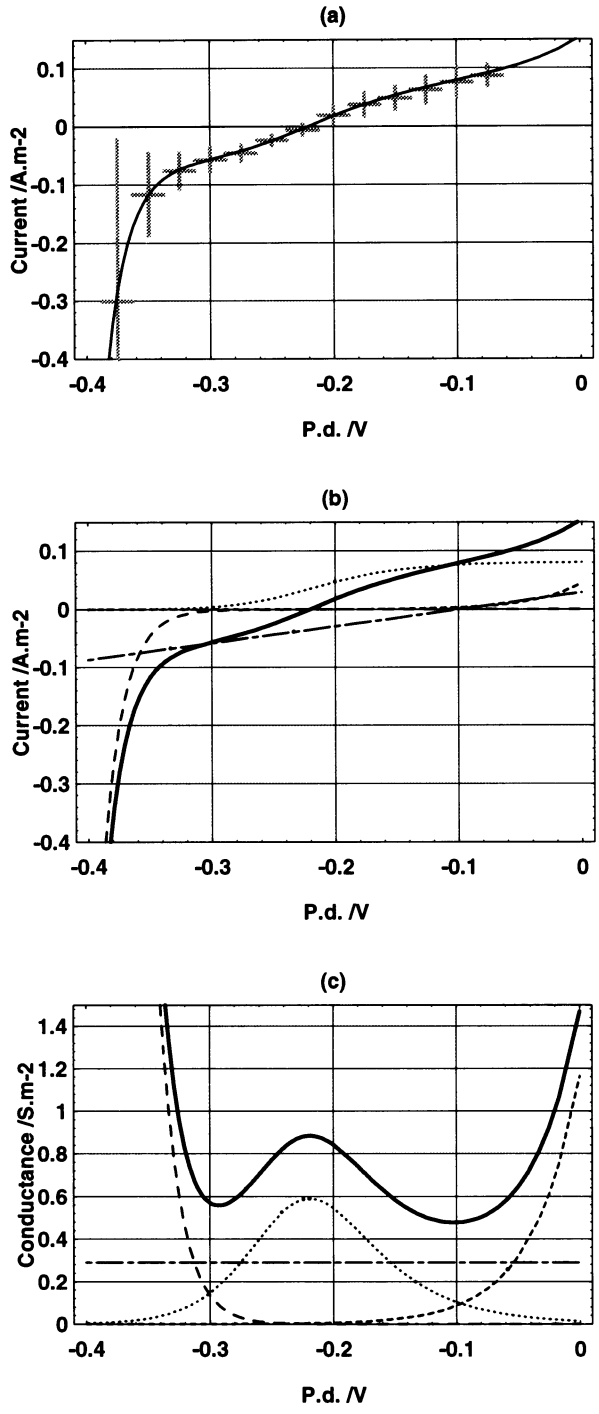

Fig. 5. (*a*)A set of 5 intact cells with voltage clamp applied to plasmalemma only. The data has been gathered into 25 mV slots (horizontal error bars) and the standard errors are shown as the vertical bars. The line represents the *I/V* profile generated by the model. The resting p.d. is −221 ± 12 mV. (*b*) The various transport systems constituting the *I/V* profile: ····· the pump current i_p, – – – – – the background current, – – – – – the inward rectifier i_{inrec}, -------- the outward rectifier i_{outrec}. For the mathematical form *see* Materials and Methods. The parameter values can be found in Table 2. The data p.d. window was limited to ~−80 mV to avoid excitation transients. The outward rectifier fitted to another set of data has been used. *(c)* The corresponding *G/V* profiles.

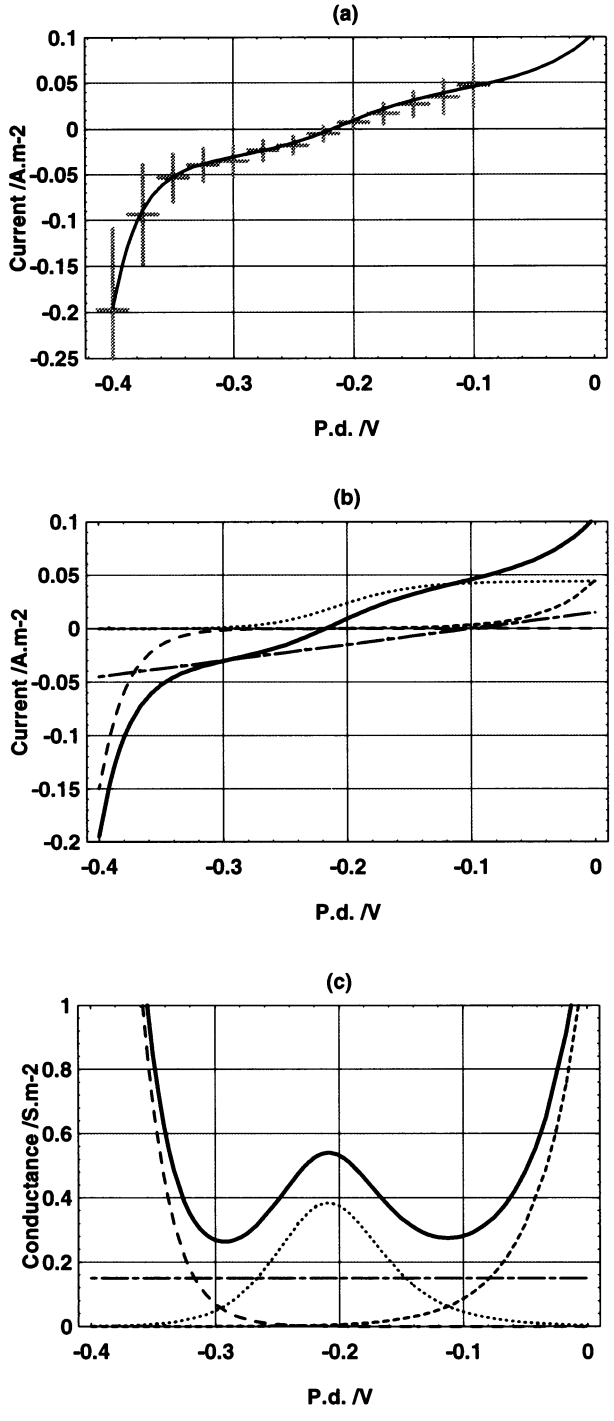

Fig. 6. (*a*) A set of 5 intact cells with voltage clamp applied to plasmalemma and tonoplast. The data has been gathered into 25 mV slots (horizontal error bars) and the standard errors are shown as the vertical bars. The line represent the *I/V* profile generated by the model. The resting p.d. is −217 ± 12 mV. (*b*) The various transport systems constituting the *I/V* profile: ····· the pump current i_p, – – – – – the background current, – – – – – the inward rectifier i_{inrec}, ---------- the outward rectifier i_{outrec}. For the mathematical form *see* Materials and Methods. The parameter values can be found in Table 2. The data p.d. window was limited to $\lesssim$−100 mV to avoid excitation transients. The outward rectifier fitted to another set of data has been used. (*c*) The corresponding *G/V* profiles.

To estimate the effect of zero turgor on the *I/V* characteristics data from 7 cells with their ends cut, but retaining their cytoplasm, were analysed (*see* Fig. 7). The resting p.d. was depolarized at −169 ± 12 mV, but the *I/V* profile was similar to those observed in the intact cells (in this case plasmalemma and tonoplast were voltage clamped, so comparison to the data in Fig. 6 is more appropriate).

The cells perfused with ATP fell into three groups: hyperpolarized group with resting p.d. −175 ± 12 mV (4 cells) and *I/V* profile similar to the intact and cut unperfused cells (Fig. 8); depolarized group with resting p.d. of −107 ± 12 mV (6 cells) and *I/V* profiles close to linear (Fig. 9); and excited cells with profiles showing a negative conductance region and resting p.d. at −59 ± 12 mV (5 cells, *see* Fig. 10). The cells perfused with medium containing no ATP showed upwardly concave *I/V* characteristics and resting p.d.s at −81 ± 12 mV (6 cells, *see* Fig. 11).

Some sets of data did not extend far enough to fit either i_{outrec} (in these cells excitation transients would have made the *I/V* curve difficult to interpret) or i_{inrec}. These sets of data are marked by ''*'' (i_{outrec}) or ''**'' (i_{inrec}) in Table 2 and a fit from another data set is used for completeness.

Discussion

The Effect of Perfusion on the *I/V* Characteristics

The shapes of the *I/V* profiles are similar for the cytoplasmic and vacuolar voltage clamps (Figs. 5 and 6). They are also similar to earlier results (Beilby, 1984; Fig. 2). A comparison of the parameters in Table 2 shows that the vacuolar voltage clamp data yield a higher value for the pump parameter k^0_{oi}, lower value for the pump parameter κ_{oi} and lower background conductance. These findings indicate, that it is important to voltage-clamp the plasmalemma alone for accurate results, but an approximate indication of parameter values can be obtained by clamping both plasmalemma and tonoplast in series.

The unperfused, cut cells (Fig. 7) indicate the effect of zero turgor on the *I/V* profile (as both the membranes are still in place, these data must be compared to the vacuolar clamp profile). From Table 2, we can see that both the voltage-dependent pump parameters have been affected: k^0_{io} decreasing and k^0_{oi} increasing. The voltage-independent pump parameter κ_{oi} also decreased and background conductance increased. If the simulated background conductance is decreased to the intact cell level (Table 2), the resting p.d. hyperpolarizes to −186 mV, still more depolarized than that in the intact cells. This depolarization suggests some direct effect of zero turgor on the pump parameters.

Table 2. Parameter values

Data set	E_m	Pump				i_{outrec}		i_{inrec}		g background	E_p
		k^0_{io}	k^0_{oi}	κ_{io}	κ_{oi}	k_1	k_2	c_1	c_2		
	mV		s^{-1}						$S.m^{-2}$	mV	
Blatt, Beilby and Tester (1990) (pH 7.5)	−230	5920	0.11	0.085	102					~0.3	−457
Cytoplasm intact cells Fig. 5	−221	5000	0.5	0.1	42	26	1.5*	60	18.8	0.29	−383
Vacuole intact cells Fig. 6	−217	5000	1.05	0.1	23	26	1.5*	46	15	0.15	−349
Vacuole cell ends cut Fig. 7	−169	2500	1.6	0.1	15	26	1.5*	41	14.5	0.25	−310
Perfused cells + ATP, hyperpol. Fig. 8	−175	1000	1.4	0.1	18	26	1.5*	46	14.5	0.22	−322
Perfused cells + ATP, depol. Fig. 9	−107	50	10.0	1.0	20	26	1.5	38	10.8	0.52	−116
		no pump				21	1.9	38	10.8	0.55	
		Excitation current									
		a	t_1	t_2	u_1	u_2					
Excited cells +ATP Fig. 10	−59	0.133	17.3	2.0	11.5	2.0	26	2.8	38	10.8**	0.65	
No ATP Fig. 11	−81	0.015	17.0	2.0	11.5	2.0	26	1.8	41	10.4	0.3	

E_m is the average resting p.d. for each data set (*see* text for standard error). E_p is the pump reversal p.d. calculated from the two-state HGSS model for the shown set of parameters. The data sets marked with * did not extend far enough to fit i_{outrec}. Here we used k_1 and k_2 fitted to depolarized cells perfused with +ATP (Fig. 9). The data set marked with ** did not extend far enough to fit i_{inrec}. Here we used c_1 and c_2 fitted to depolarized cells perfused with +ATP (Fig. 9).

The hyperpolarized cells perfused with ATP (Fig. 8) can be compared with the cytoplasmic clamp data, as the tonoplast has been washed away in the perfusion process. The changes show similar trend to the effect of zero turgor: k^0_{io} and κ_{oi} diminish and k^0_{oi} increases. The background conductances are similar.

The depolarized cells perfused with ATP (Fig. 9) show a linear *I/V* profile in the p.d. window: −280 to −80 mV. Consequently, either there is a drastic decrease in k^0_{io}, which moves the conductance maximum into the i_{outrec} region (such as shown in Fig. 9) or, alternatively, the pump contribution becomes too small to be observed. The data can be fitted satisfactorily by the same i_{inrec}, no pump current and slightly different background current and i_{outrec} (*see* Table 2). Such diminishing of the pump current would occur via the decrease in parameter κ_{oi} (*see* Fig. 4). The ''no pump'' alternative is more likely for this set of data, as the pump reversal p.d. of −116 mV is too depolarized compared to the −500 mV ceiling estimated for the $1H^+/1$ ATP stoichiometry.

The excited cells (Fig. 10) display a large inward current, which is described by Eq. (5). The background conductance in these cells is higher than in the previous data (*see* Table 2) and it is assumed that this was the primary cause for the membrane p.d. to depolarize above the excitation threshold. In intact cells the threshold is ~−120 mV (Beilby & Coster, 1979), but in perfused cells it tends to be more depolarized (Beilby, Mimura & Shimmen, 1993). The data has been modeled without the pump. The p.d.-dependence and the amplitude of the

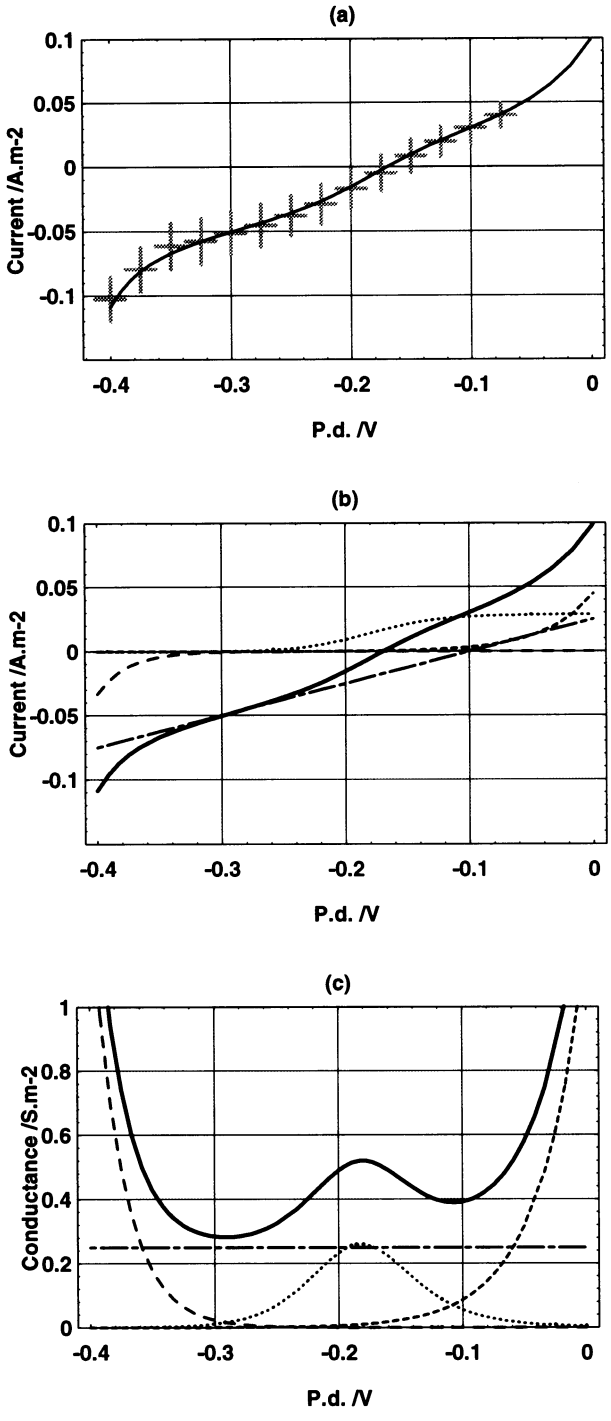

Fig. 7. (*a*) A set of 7 cells with the ends amputated, but with their original cytoplasm still in place. (voltage clamp applied to plasmalemma and tonoplast). The data has been gathered into 25 mV slots (horizontal error bars) and the standard errors are shown as the vertical bars. The line represents the *I/V* profile generated by the model. The resting p.d. is −169 ± 12 mV. (*b*) The various transport systems constituting the *I/V* profile: ····· the pump current i_p, – – – – – the background current, – – – – – the inward rectifier i_{inrec}, ---------- the outward rectifier i_{outrec}. For the mathematical form *see* Materials and Methods. The parameter values can be found in Table 2. The data p.d. window was limited to ~−80 mV to avoid excitation transients. The outward rectifier fitted to another set of data has been used (*c*) The corresponding *G/V* profiles.

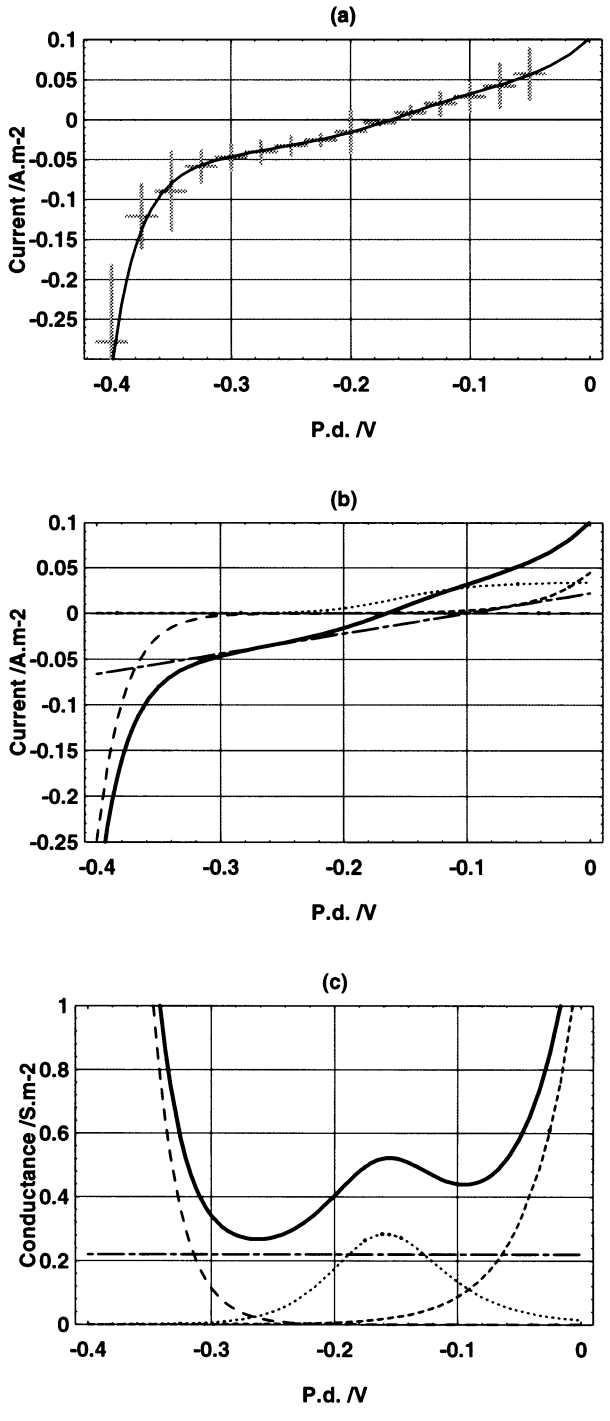

Fig. 8. (*a*) A set of 4 cells perfused with +ATP medium (*see* Table 1 for composition). The data have been gathered into 25 mV slots (horizontal error bars) and the standard errors are shown as the vertical bars. The line represents the *I/V* profile generated by the model. The resting p.d. is −175 ± 12 mV. (*b*) The various transport systems constituting the *I/V* profile: ····· the pump current i_p, – – – – – the background current, – – – – – the inward rectifier i_{inrec} ---------- the outward rectifier i_{outrec}. For the mathematical form *see* Materials and Methods. The parameter values can be found in Table 2. The data p.d. window was limited to ~−50 mV to avoid excitation transients. The outward rectifier fitted to another set of data has been used. (*c*) The corresponding *G/V* profiles.

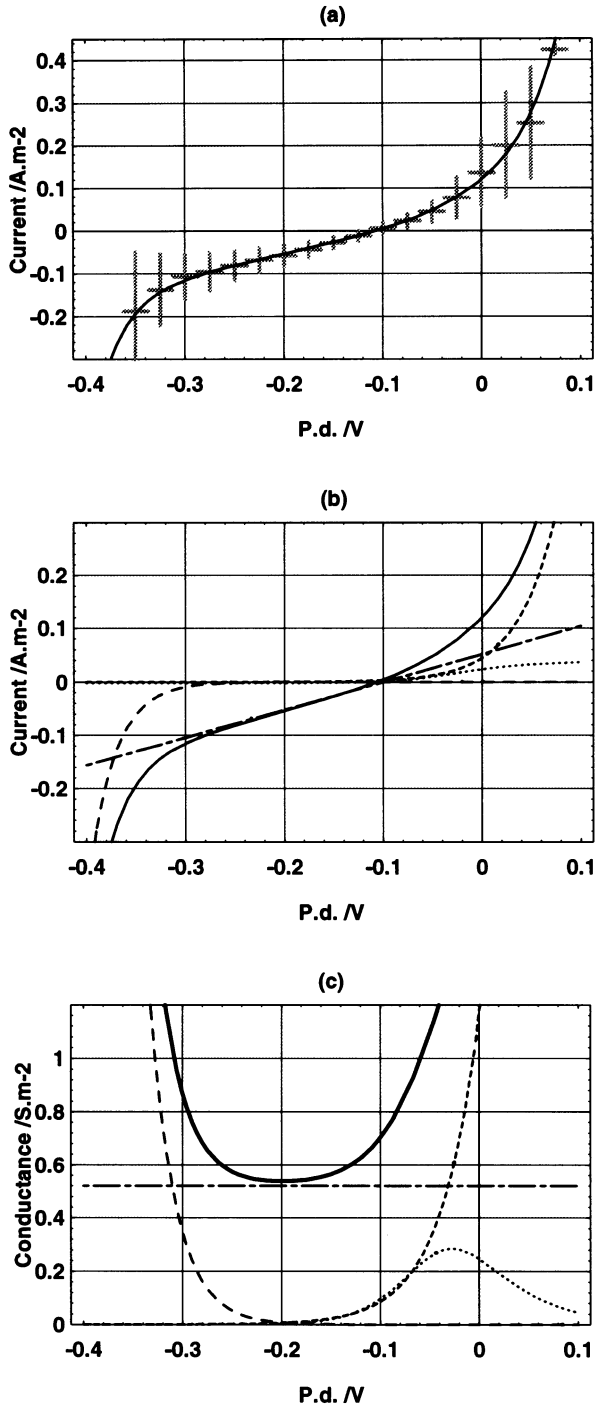

Fig. 9. (*a*) A set of 6 cells perfused with +ATP medium (*see* Table 1 for medium composition), showing a depolarized resting p.d. of −107 ± 12 mV. The data has been gathered into 25 mV slots (horizontal error bars) and the standard errors are shown as the vertical bars. The line represents the *I/V* profile generated by the model. (*b*) The various transport systems constituting the *I/V* profile: ····· the pump current i_p, – – – – – the background current, – – – – the inward rectifier i_{inrec}, - - - - - - the outward rectifier i_{outrec}. For the mathematical form *see* Materials and Methods. The parameter values can be found in Table 2. (*c*) The corresponding *G/V* profiles.

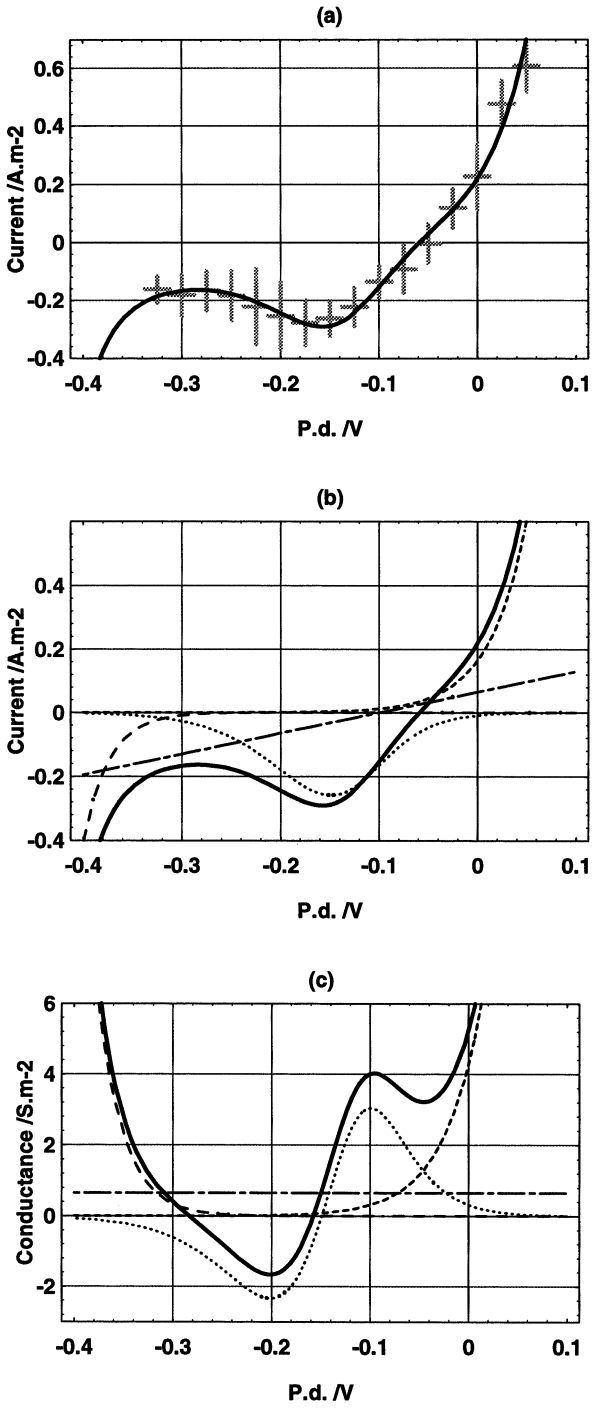

Fig. 10. (*a*) A set of 5 cells perfused with +ATP medium showing the excited state with a resting p.d. of −59 ± 12 mV. The data has been gathered into 25 mV slots (horizontal error bars) and the standard errors are shown as the vertical bars. The line represents the *I/V* profile generated by the model. (*b*) The various transport systems constituting the *I/V* profile: ····· the inward current i_{excit}, – – – – – the background current, – – – – – the inward rectifier i_{inrec}, ---------- the outward rectifier i_{outrec}. For the mathematical form *see* Materials and Methods. The parameter values can be found in Table 2. (*c*) The corresponding *G/V* profiles.

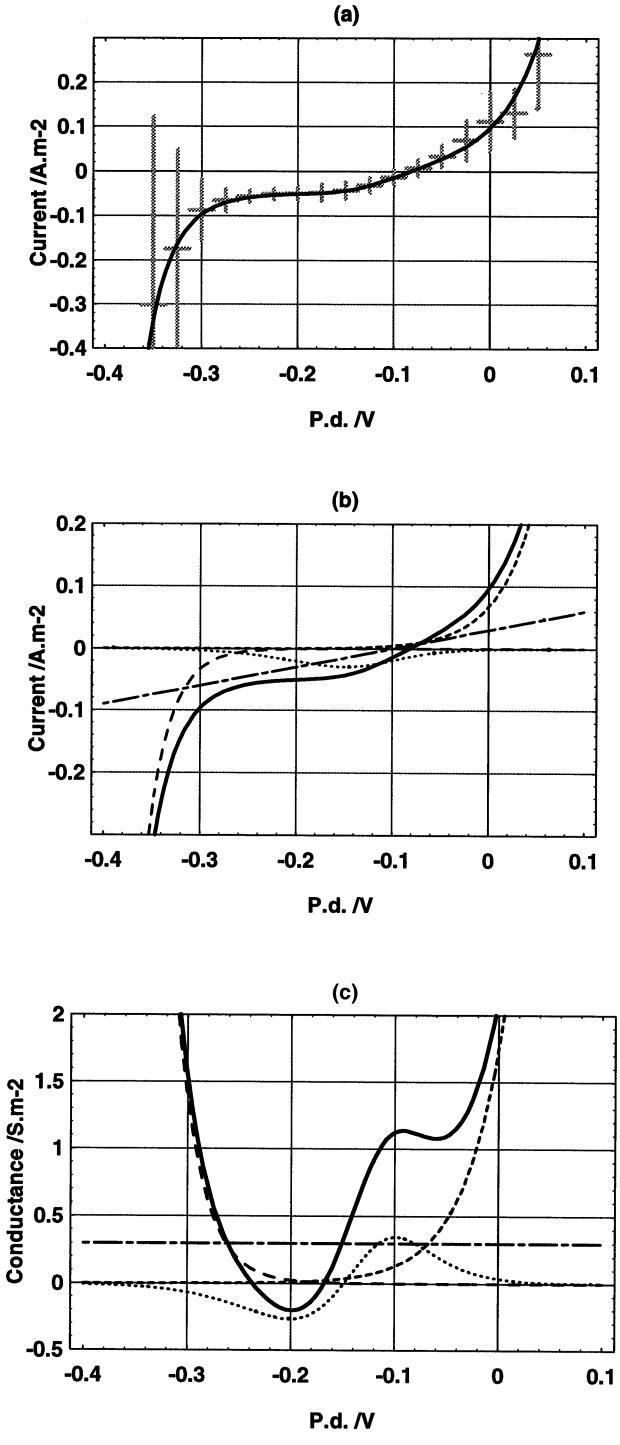

Fig. 11. (*a*) A set of 6 cells perfused with −ATP medium (*see* Table 1 for medium composition). The resting p.d. was −81 ± 12 mV. The data has been gathered into 25 mV slots (horizontal error bars) and the standard errors are shown as the vertical bars. The line represents the *I/V* profile generated by the model. (*b*) The various transport systems constituting the *I/V* profile: ····· the inward current $i_{no\text{-}ATP}$, – – – – – the background current, ——— the inward rectifier i_{inrec}, ---------- the outward rectifier i_{outrec}. For the mathematical form *see* Materials and Methods. The parameter values can be found in Table 2. (*c*) The corresponding *G/V* profiles.

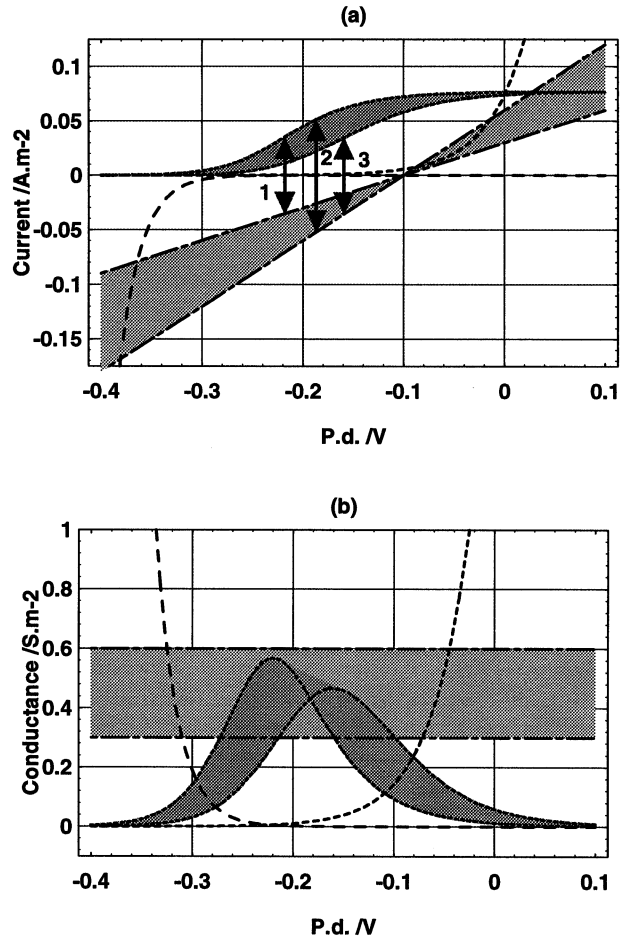

Fig. 12. A scheme for the membrane resting p.d. in terms of the *I/V* (*a*) and *G/V* (*b*) profiles of various transporters: ····· the pump current i_p, – – – – – the background current, – – – – – – the inward rectifier i_{inrec}, ---------- the outward rectifier i_{inrec}. The shaded regions connect two background currents with different conductances and an increase in the k^0_{io} pump parameter, which determines the position of the conductance maximum. The arrows in (*a*) signify the ''zero current'' for various combinations of current profiles (for the values of the resting p.d., *see* text).

inward current makes it difficult to determine whether the pump is present.

Cells perfused without ATP were modeled with the linear background current, inward current, $i_{no\text{-}ATP}$, (*see* Eq. (6)) and i_{inrec} and i_{outrec} (Fig. 11). The background conductance in this case is close to that in intact cells (cytoplasmic voltage clamp) and hyperpolarized perfused cells. The p.d. dependence of the inward current is very similar to that of i_{excit}, but the amplitude is about an order of magnitude smaller (*see* Table 2).

The inward and outward rectifiers showed a large scatter in most of the cell populations. However, each set of data could be satisfactorily fitted with an exponential curve. The present data did not indicate consistent effect of either zero turgor nor ATP withdrawal.

The Generation of the Resting Potential

From looking at Table 2, we can reach some interesting conclusions about the way resting p.d. is controlled by the ensemble of the various transport systems. In Fig. 12, let us consider the less conductive background current (top of the background current shaded region) and the more conductive pump *I/V* profile (top of the pump current shaded region). The resting p.d. is determined by the zero current: in Fig. 12*a* it is set by the background and the pump currents (at −218 mV) when they are equal and opposite in magnitude, as shown by arrow ''1.'' If the background current becomes more conductive (bottom of the background current shaded region), the resting potential will move toward its zero current potential, E_B, as shown by arrow ''2,'' depolarizing the p.d. to −190 mV. The pump parameter k_{io}^0 was previously defined to be independent of p.d. (the p.d. dependence of the pump is provided by the exponential part of equations 1*a,b*). However, the results in Table 2 suggest that this parameter tends to diminish, if the resting p.d. is forced to more depolarized levels by, for instance, an increased background conductance, opening of the K^+ channels or (in perfused cells) by the excitation current. Experiments with prolonged voltage clamping to depolarized p.d. levels (M.J. Beilby, *in preparation*) support this assumption and suggest that the exposure to low p.d.s must be in order of minutes to affect k_{io}^0. Consequently, a positive feedback loop might be set up by the initial increase of the background conductance: p.d. depolarizes, this in turn diminishes k_{io}^0, which in turn depolarizes the membrane more (to −159 mV, arrow ''3,'' Fig. 12*a*). Note that the pump influences the resting p.d. by changing its *I/V* profile rather than by large changes in E_p (*see* the legend of Fig. 1 for E_p values). As k_{io}^0 reaches low values (~500 sec^{-1}), the conductance maximum starts to depolarize faster (*see* Fig. 1) and becomes ''swamped'' by the large outward rectifier current. However, at such values of k_{io}^0 the pump reversal p.d. becomes too depolarized (*see* Table 2) to be consistent with the values predicted by the 1 H^+ per 1 ATP stoichiometry. It is then more likely that the pump current diminishes below observable levels. (Note that the data sets with low p.d. values shown in Figs. 9 and 10 give no clear evidence of the pump currents or conductance).

The modeling of the various transporters also allows us to determine if the inward rectifier plays an important part in setting of the resting p.d. (as suggested by Tyerman, Findlay and Paterson, 1986*b*). In Fig. 12*a*, the inward rectifier does not contribute to resting p.d. determination. However, if the background current became less conductive, or, if the inward rectifier moved in positive direction (as it does with decreasing pH, Tyerman, Findlay & Paterson, 1986*b*), the resting p.d. might be influenced by it.

The Inward Currents, I_{excit} and $I_{no\text{-}ATP}$

The presence of ATP is also required for the excitation currents to flow, although much less ATP is necessary to sustain the excitation state than the hyperpolarized pump state (Mimura, Shimmen & Tazawa, 1983). In intact *Chara* cells large transient currents occur for the p.d. levels more depolarized than ~ −120 mV (Beilby & Coster, 1979). In perfused ligated cells the excitation currents are only weakly time dependent (Beilby, Mimura & Shimmen, 1993) and the *I/V* curves display a negative conductance region similar to that observed with cells in K^+ state (Beilby, 1985). In Fig. 13 the resting p.d. (−59 mV) is determined by the balance of the outward rectifier current, the background current and the excitation current, as shown by the arrow ''1.'' Note that the i_{excit} (Fig. 13*b*) is always negative: the reversal p.d. seems to be outside the channel high open probability p.d. window. This possibility is often neglected when the channels are identified by modification of the concentrations on one or both sides of the membrane. If the excitation current is carried mainly by Cl^- and $[Cl^-]_o$ is increased, the current amplitude probably increases as well (compare with the behavior of the K^+ channels — Beilby, 1985), but the reversal potential E_{Cl} can be still out of the channel high open probability window. Thus the cell p.d. would depolarize despite E_{Cl} becoming less positive. Such an effect was seen by Shiina and Tazawa (1987) and taken as an indication that the inward current is not carried by Cl^-.

The *I/V* curve without ATP is not the expected linear background profile, but upwardly concave curve. The close similarity in p.d.-dependence of i_{excit} and $i_{no\text{-}ATP}$ (compare Eq. (5) and (6), parameters in Table 2 and *see* Fig. 13) suggests that they are closely related. The resting p.d. (−81 mV) is set by balancing the background current, $i_{no\text{-}ATP}$ and i_{outrec}. The influence of ATP on channels was suggested by Smith and Walker (1981) and Mimura, Shimmen and Tazawa (1983). Katsuhara, Mimura and Tazawa (1990) observed a poorly selective K^+ channel in plasmalemma of *Nitellopsis obtusa*, which showed an increase in open probability upon withdrawal of ATP. However, the channels that we observe pass an inward current and are more likely to be Cl^- channels. The main difference between the excited and the no-ATP states is the greater amplitude of the excitation current, which makes the negative conductance region more apparent (*see* Fig. 13). What is the mechanism which converts i_{excit} into $i_{no\text{-}ATP}$? Thiel, Homann and Gradmann (1993) found two types of Cl^- channels that are more likely to open at depolarized p.d. levels. The decrease in amplitude of the inward current in no-ATP systems could arise from one or more combinations of Cl^- channels: type of Cl^- channel which is ATP-dependent (such as, for instance, the Cl^- transporter CFTR, Hyde et al., 1990) or inactivated by prolonged depolarization. Yao,

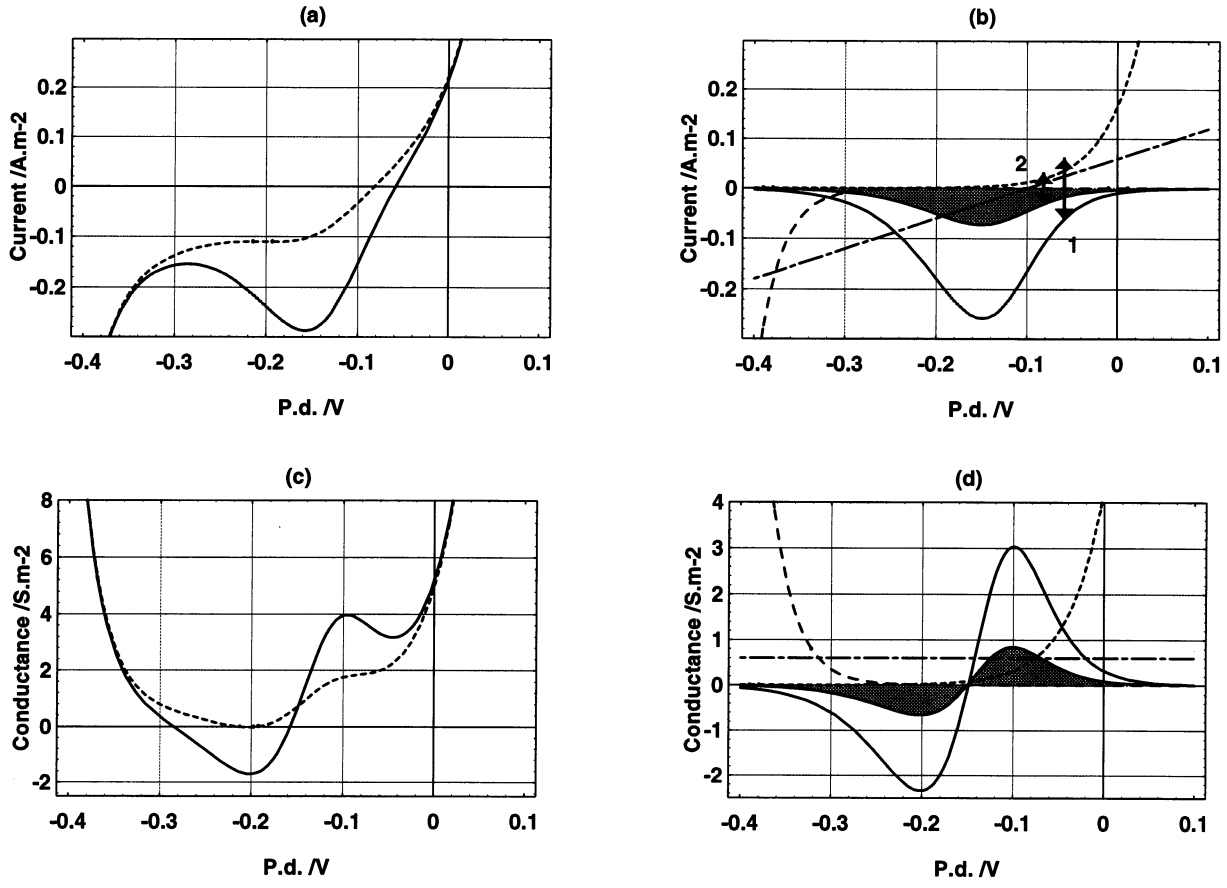

Fig. 13. Modeling the total current (*a*) and conductance (*c*) in the excited state (perfused cells) ———— and no-ATP state ----------. The separate currents are shown in (*b*) and the conductances in (*d*). The profiles have been obtained by combining the inward rectifier current i_{inrec}, – – – – –, the outward rectifier current i_{outrec} ----------, the background current – - - - – and the excitation current ————, or no-ATP current (shaded regions). The equations are given in Materials and Methods and the parameters in Table 2. The arrows ''1'' and ''2'' show the zero current (for the values *see* text) for each state. Note that the outward rectifier participates in setting of the resting p.d. level.

Bisson and Brzezicki (1992) applied DES and vanadate to *Chara corallina* and *Chara buckellii* (*longifolia*) cells perfused with 4 mM ATP. The vanadate (+ATP) *I/V* profile was very close to the no-ATP profile in both materials, both showing upwardly concave curvature. The DES (+ATP) *I/V* profiles were more linear. This effect supports our hypothesis that $i_{\text{no-ATP}}$ is associated with excitation: vanadate inactivates the proton pump, but does not depress excitation (Shimmen and Tazawa, 1982); DES inactivates the pump and removes excitable currents (obviously not via ATP depletion) and consequently the DES-revealed current is close to the linear background current. Ca^{++} activated anion channels in guard cells exhibit similar behavior as a function of ATP concentration (Hedrich, Busch & Raschke, 1990).

Another scenario for the conversion of i_{excit} to $i_{\text{no-ATP}}$ is the total inactivation of the Cl^- channels by the lack of ATP, thus revealing the elusive Ca^{++} channels.

Conclusion

The modeling of the total *I/V* characteristics of *Chara* furnished information about the parameters of the Two-state HGSS pump model and revealed that the cells with no ATP display an extra transport system, which is very similar to the excitation state. The fitting of this model to the total *I/V* characteristics of the membrane is a starting point to a large scale investigation. The p.d.- and time-dependence of the Two-state pump parameter k^0_{io} is currently being studied using the voltage clamp. The data on the effect of acidification of cytoplasm (e.g., by butyric acid) will be simulated by the model. The effects of the concentrations of ADP and P_i in the cytoplasm (which are thought to be subsumed by the parameter κ_{io}, Blatt, Beilby & Tester, 1990) can be fitted by the model. The rectifier currents will be modeled with Eyring-barrier type expressions and compared to data obtained from patch clamp studies. Modeling the effects of changing concentrations of the major ions in the medium can also give us further clues to the identity of the background current. Application of Cl^- or Ca^{++} blockers will identify $i_{\text{no-ATP}}$.

To construct detailed models of the channels and the pump, it will be necessary for the underlying proteins to be sequenced and the active branches identified by ge-

netic engineering. The protein molecule can then be overlaid by regions of fixed charge as in the case of the KAT1 channel (Chilcott et al., 1995).

The experiments in this paper have been performed while MJB was employed on NAWs Australian Research Council grant, which is gratefully acknowledged. We thank Dr. M. Bisson for critical reading of the manuscript. Part of this work has been presented as a poster at 10th International Workshop on Plant Membrane Biology in Regensburg, August, 1995.

References

Beilby, M.J. 1984. Current-voltage characteristics of the proton pump at *Chara* plasmalemma: I. pH dependence. *J. Membrane Biol.* **81:**113–125

Beilby, M.J. 1985. Potassium channels at *Chara* plasmalemma. *J. Exp. Bot.* **36:**228–239

Beilby, M.J. 1986. Factors controlling the potassium conductance in *Chara. J. Membrane Biol.* **93:**187–193

Beilby, M.J. 1989. Transport systems at *Chara* plasmalemma. *In:* Plant Membrane Transport: The Current Position, J. Dainty, M.I. de Michelis, E. Marre and F., editors. pp. 31–34. Rasi-Caldogno, Elsevier, Amsterdam

Beilby, M.J. 1990. Current-voltage curves for plant membrane studies: A critical analysis of the method. *J. Exp. Bot.* **41:**165–182

Beilby, M.J., Beilby, B.N. 1983. Potential dependence of the admittance of *Chara* plasmalemma. *J. Membrane Biol.* **74:**229–245

Beilby, M.J., Coster, H.G.L. 1979. The action potential in *Chara corallina* II. Two activation-inactivation transients in voltage clamps of the plasmalemma. *Aust. J. Plant Physiol.* **6:**323–325

Beilby, M.J. MacRobbie, E.A.C. 1984. Is calmodulin involved in electrophysiology of *Chara corallina? J. Exp. Bot.* **35:**568–580

Beilby, M.J., Mimura, T., Shimmen, T. 1993. The proton pump, high pH channels, and excitation: voltage clamp studies of intact and perfused cells of *Nitellopsis obtusa. Protoplasma* **175:**144–152

Beilby, M.J., Mimura, T., Shimmen, T. 1996. Perfusion: A critical analysis of the method. *J. Exp. Bot.* (*in press*)

Blatt, M.R. 1986. Interpretation of steady-state current-voltage curves: consequences and implications of current subtraction in transport studies. *J. Membrane Biol.* **92:**91–110

Blatt, M.R. 1987. Electrical characteristics of stomatal guard cells: the contribution of ATP-dependent, ''electrogenic'' transport revealed by current-voltage and difference-current-voltage analysis. *J. Membrane Biol.* **98:**257–274

Blatt, M.R., Beilby, M.J., Tester, M. 1990. Voltage dependence of the *Chara* proton pump revealed by current-voltage measurement during rapid metabolic blockade with cyanide. *J. Membrane Biol.* **114:**205–223

Chapman, J.B., Johnson, E.A., Kootsey, J.M. 1983. Electrical and biochemical properties of an enzyme model of the sodium pump. *J. Membrane Biol.* **74:**139–153

Chilcott, T.C., Frost Shartzer, S., Iverson, M.W., Garvin, D.F., Kochian, L.V., Lucas, W.J. 1995. Potassium transport kinetics of KAT1 expressed in *Xenopus* oocytes: a proposed molecular structure and field effect mechanism for membrane transport. *C.R. Acad. Sci. Paris* **318:**761–771

Fisahn, J., Hansen U.-P., Lucas, W.J. 1992. Reaction kinetic model of a proposed plasma membrane two-cycle H^+-transport system of *Chara corallina, Proc. Natl. Acad. Sci. USA* **89:**3261–3265

Fisahn, J., Lucas W.J. 1992. Direct measurement of the reversal potential and current-voltage characteristics in the acid and alkaline regions of *Chara corallina. Planta* **186:**241–248

Hansen, U.-P., Gradmann, D., Sanders, D., Slayman, C.L. 1981. Interpretation of current-voltage relationships for ''active'' ion transport systems: I. Steady-state reaction-kinetic analysis of class-I mechanisms. *J. Membrane Biol.* **63:**165–190

Hedrich, R., Busch, H., Raschke, K. 1990. Ca^{++}- and nucleotide-dependent regulation of voltage-dependent anion channels in the plasma membrane of guard cells. *EMBO J.* **9:**3889–3892

Hope, A.B., Walker, N.A. 1975. The Physiology of Giant Algal Cells. Cambridge University Press, London

Hyde, C., Emsley, P., Hartshorn, M.J., Mimmack, M.M., Gileadi, U., Pearce, S.R., Gallagher, M.P., Gill, D.R., Hubbard, R.E., Higgins, C.E. 1990. Structural model of ATP-binding proteins associated with cystic fibrosis, multidrug resistance and bacterial transport. *Nature* **346:**362–365

Katsuhara, M., Mimura, T., Tazawa, M. 1990. ATP-regulated ion channels in the plasma membrane of a characeae alga, *Nitellopsis obtusa. Plant Physiol.* **93:**343–346

Kishimoto, U., Kami-ike, N., Takeuchi, Y., Ohkawa, T. 1984. A kinetic analysis of the electrogenic pump of *Chara corallina:* I. Inhibition of the pump by DCCD. *J. Membrane Biol.* **80:**175–183

Mimura, T., Shimmen, T., Tazawa, M. 1983. Dependence of the membrane potential on intracellular ATP concentration in tonoplast-free cells of *Nitellopsis obtusa. Planta* **157:**97–104

Schroeder, J.I. 1989. Quantitative analysis of outward rectifying K^+ channel currents in guard cell protoplasts from *Vicia faba. J. Membrane Biol.* **107:**229–235

Shepherd, V.A., Goodwin, P.B. 1992. Seasonal patterns of cell-to cell communication in *Chara corallina* Klein ex Willd. I. Cell-to-cell communication in vegetative lateral branches during winter and spring. *Plant Cell Environ.* **15:**137–150

Shiina, T., Tazawa, M. 1987. Demonstration and characterization of Ca^{2+} channel in tonoplast-free cells of *Nitellopsis obtusa. J. Membrane Biol.* **96:**263–276

Shimmen, T., Tazawa, M. 1982. Effects of intracellular vanadate on electrogenesis, excitability and cytoplasmic streaming in *Nitellopsis obtusa. Plant Cell Physiol* **23:**669–677

Smith, P.T., Walker N.A. 1981. Studies on the perfused plasmalemma of *Chara corallina:* I. Current-voltage curves: ATP and potassium dependence. *J. Membrane Biol.* **60:**223–236

Smith, J.R., Walker, N.A., Smith, F.A. 1987. Potassium transport across the membranes of *Chara.* III. Effects of pH, inhibitors and illumination. *J. Exp. Bot.* **38:**778–787

Takeuchi, Y., Kishimoto, U., Ohkawa, T., Kami-ike, N. 1985. A kinetic analysis of the electrogenic pump of *Chara corallina:* II. Dependence of the pump activity on external pH. *J. Membrane Biol.* **86:**17–26

Terry, B.R., Tyerman, S.D., Findlay, G.P. 1991. Ion channels in the plasma membrane of *Amaranthus* protoplasts: One cation and one anion channel dominate the conductance. *J. Membrane Biol.* **121:**223–236

Thiel, G. Homann, U., Gradmann, D. 1993. Microscopic elements of electrical excitation in *Chara:* Transient activity of Cl^- channels in the plasma membrane. *J. Membrane Biol.* **134:**53–66

Tsutsui I., Ohkawa T. 1993. N-Ethylmaleimide blocks the H^+ pump in the plasma membrane of *Chara corallina* internodal cells. *Plant Cell Physiol.* **34:**1159–1162

Tyerman, S.D., Findlay, G.P., Paterson, G.J. 1986*a.* Inward membrane current in *Chara inflata.* I. A voltage- and time-dependent component. *J. Membrane Biol.* **89:**139–152

Tyerman, S.D., Findlay, G.P., Paterson, G.J. 1986*b.* Inward membrane current in *Chara inflata.* I. Effects of pH, Cl^- -channel blockers and NH^+_4, and significance for the hyperpolarized state. *J. Membrane Biol.* **89:**153–161

Yao, X., Bisson, M.A., Brzezicki, L.J. 1992. ATP-driven proton pumping in two species of *Chara* differing in salt tolerance. *Plant Cell Environ* **15:**199–210